Vol. 30 (1999) ACTA PHYSICA POLONICA B No 7

THE LHCb EXPERIMENT*

Tatsuya Nakada

CERN, CH-1211 Geneva 23, Switzerland
and
PSI, CH-5234 Villigen-PSI, Switzerland

(Received May 2, 1999)

LHCb is a dedicated experiment to study CP violation and other rare phenomena in B-meson decays at LHC. The detector is design to have a particle identification system based on the RICH detectors, excellent mass and decay time resolutions and a very efficient trigger system which is sensitive to both hadronic and leptonic final states. With those properties, the experiment will be able to fully exploit the large number of different kind of B mesons produced at LHC and probe physics beyond the Standard Model.

PACS numbers: 07.05.Fb, 12.15.Hh, 13.20.He, 13.75.Cs

1. Introduction

CP violation is one of the remaining mysteries in particle physics. Although the Standard Model can accommodate the observed CP violation phenomena in the neutral kaon system, no experimental precision test has been performed which examines the consistency of the Standard Model in CP violation.

Strong interest in CP violation is not limited to particle physics. In cosmology, CP violation is one of the three necessary conditions to generate matter–antimatter asymmetry [1]. The Standard Model however does not seem to be able to generate sufficient CP violation so that the universe could be dominated by matter as it is now [2]. This calls for new sources of CP violation beyond the Standard Model.

In the kaon system, quantitative tests of the Standard Model in CP violation are limited mainly due to the theoretical uncertainties. The presence of large hadronic effects in the process makes precise Standard Model predictions very difficult.

* Presented at the XXVII International Meeting on Fundamental Physics, Sierra Nevada, Granada, Spain, February 1–5, 1999.

In the neutral B-meson systems, there exist CP violating phenomena where the effects of strong interactions are either very small or experimentally measurable and the Standard Model can make accurate predications. There are also many more decay modes than the kaon system that exhibit CP violation, allowing various consistency tests. For these reasons, there is already an extensive experimental programme to look for CP violation in the neutral B-meson systems: BaBar, Belle, CDF, CLEO, D0 and HERA-B. However, the precision test of the Standard Model will remain by far incomplete due to the limited statistics and detector capabilities in those experiments, and the LHC will still play a crucial role in order to reveal physics beyond the Standard Model. A dedicated experiment is essential to exploit the potential of the LHC.

2. Physics case

The Cabibbo–Kobayashi–Maskawa quark mass mixing matrix [3] can be approximated as

$$V_{\rm CKM} = \begin{pmatrix} V_{ud} & V_{us} & V_{ub} \\ V_{cd} & V_{cs} & V_{cb} \\ V_{td} & V_{ts} & V_{tb} \end{pmatrix} \approx V^{(3)}_{\rm CKM} + \delta V_{\rm CKM}$$

where

$$V^{(3)}_{\rm CKM} = \begin{pmatrix} 1-\lambda^2/2 & \lambda & A\lambda^3\,(\rho - i\,\eta) \\ -\lambda & 1-\lambda^2/2 & A\lambda^2 \\ A\lambda^3\,(1-\rho-i\,\eta) & -A\lambda^2 & 1 \end{pmatrix}$$

using the Wolfenstein parameterization [4]. With this parameterization, CP violation is generated by $\eta \neq 0$ in the Standard Model. The parameter $\lambda = 0.221 \pm 0.002$ [5] is measured from light quark decays. The term $\delta V_{\rm CKM}$ includes the contributions proportional to λ^4 and λ^5 which should not be neglected for CP violation in the neutral kaon decays and high precision CP studies in the neutral B-meson decay.

A strategy to extract the rest of the parameters is the following. In order to simplify the discussion, we neglect $\delta V_{\rm CKM}$. The decay width $\Gamma_{b\to c+W}$, obtained from semileptonic B-meson decays generated by $b \to c\ell\overline{\nu}$, determines $|V_{cb}|^2$: hence A can be extracted. The decay width $\Gamma_{b\to u+W}$, obtained from semileptonic B-meson decays generated by $b \to u\ell\overline{\nu}$ determines $|V_{ub}|^2$, *i.e.*

$$\rho^2 + \eta^2 \propto \sqrt{\Gamma_{b\to u+W}}\,. \tag{1}$$

The frequency of B^0-$\overline{B}^0$ oscillations, Δm_{B^0}, is proportional to $|V_{td}|^2$ with high accuracy. *i.e.*

$$\sqrt{(1-\rho)^2 + \eta^2} \propto \Delta m_{B^0}\,. \tag{2}$$

From these two relations, ρ and η can be determined. This procedure is in the ρ–η plane and shown in figure 1.

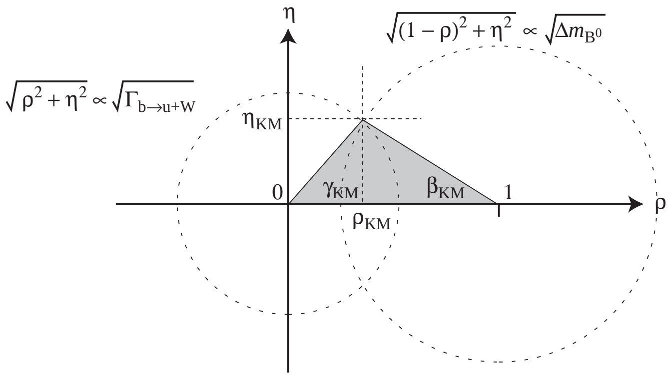

Fig. 1. Illustration of how the CKM parameters ρ and η are determined from $b \to u\ell\overline{\nu}$ decays and B^0–$\overline{B}^0$ oscillations.

A unique solution $(\rho_{\rm KM}, \eta_{\rm KM})$, where $\eta_{\rm KM} > 0$, is obtained once we assume that observed CP violation in the neutral kaon system is due to the Standard Model. The phase of V_{td} and V_{ub} is then

$$\arg V_{td} = -\beta_{\rm KM}, \quad \arg V_{ub} = -\gamma_{\rm KM},$$

where $\beta_{\rm KM}$ and $\gamma_{\rm KM}$ are determined as

$$\beta_{\rm KM} = \tan^{-1}\frac{\eta_{\rm KM}}{1-\rho_{\rm KM}}, \quad \gamma_{\rm KM} = \tan^{-1}\frac{\eta_{\rm KM}}{\rho_{\rm KM}}$$

as shown in the figure. It follows that the phase of the B^0–$\overline{B}^0$ oscillation amplitude is given by $\arg H_{B_d\overline{B}_d} = \arg V_{td}^2 = -2\beta_{\rm KM}$.

Both B^0 and $\overline{B}^0$ can decay into $J/\psi K_S$. Thus, a B^0 at $t = 0$ decays into $J/\psi K_S$ at time t by remaining as B^0 or oscillating first to $\overline{B}^0$. As is well known [6], the phase difference between the two processes generates CP violation. Since V_{cb} has no phase in the Wolfenstein parameterization, the phase of the B^0–$\overline{B}^0$ oscillation amplitude can be extracted from the CP asymmetry between the initial B^0 and $\overline{B}^0$ decaying into $J/\psi K_S$.

A consistency test of the CKM matrix can then be made by comparing $-2\beta_{\rm KM}$ determined from $\rho_{\rm KM}$ and $\eta_{\rm KM}$ with the phase of the B^0–$\overline{B}^0$ oscillation amplitude obtained by the CP asymmetry in B^0 and $\overline{B}^0 \to J/\psi K_S$ decays.

How does this consistency test look like in the presence of physics beyond the Standard Model? Varieties of new physics introduce new flavour changing neutral currents. While they contribute little to semileptonic decays, the B^0–$\overline{B}^0$ oscillation can be quite affected. The oscillation frequency then receives two contributions, one from the Standard Model and the other from new physics. If we still extract ρ and η using equations 1 and 2, the solution $(\tilde{\rho}, \tilde{\eta})$ no longer corresponds to that of the Standard Model, $(\rho_{\rm KM}, \eta_{\rm KM})$. The angles $\tilde{\beta}$ and $\tilde{\gamma}$ calculated in a similar way as $\beta_{\rm KM}$ and $\gamma_{\rm KM}$ using $\tilde{\rho}$ and $\tilde{\eta}$ do not give the phases of V_{td} and V_{ub}.

Since the $b \to c+W$ decay is hardly affected by new physics, CP violation in $B^0 \to J/\psi K_S$ decays still measures the phase of the B^0–$\overline{B}^0$ oscillation amplitude. The contribution from the new flavour changing neutral current in the oscillation could be complex. The phase of the oscillation amplitude then deviates from the Standard Model prediction of $-2\beta_{\rm KM}$. However, this phase measured from the CP asymmetry in B^0 and $\overline{B}^0 \to J/\psi K_S$ decays could still accidentally agree with $-2\tilde{\beta}$ determined from $\tilde{\rho}$ and $\tilde{\eta}$ within the measurement errors. In this case, although new physics is present, it will not be noticed.

This situation could be resolved, if a CP violation effect is measured in B^0 and $\overline{B}^0$ decaying into $D^{*+}n\pi$ and $D^{*-}n\pi$, *i.e.* four time-dependent decay rates. In the Standard Model, these decay modes provide $2\beta_{\rm KM} + \gamma_{\rm KM}$, and together with the $J/\psi K_S$ decay mode $\gamma_{\rm KM}$ can be extracted. Even new physics is present, which cannot be discovered by the $J/\psi K_S$ decay mode, the same procedure extracts $\gamma_{\rm KM}$. A comparison of this $\gamma_{\rm KM}$ with $\tilde{\gamma}$ obtained from the ρ–η determination will then reveal new physics.

The B_s-meson system provides further interesting information. In the Standard Model, the B_s–$\overline{B}_s$ oscillation frequency, Δm_{B_s}, determines $A^2\lambda^4$, *i.e.* it does not provide any information on ρ and η. However, the hadronic uncertainty in the determination of $(1-\rho)^2+\eta^2$ can be drastically reduced by using the ratio $\Delta m_{B^0}/\Delta m_{B_s}$. The phase of the B_s–$\overline{B}_s$ oscillation amplitude is given by $\arg H_{B_s\overline{B}_s} = 0$ when neglecting $\delta V_{\rm CKM}$ (and $2\delta\gamma_{\rm CKM}$ where $\delta\gamma_{\rm KM} = \tan^{-1}\lambda^2\eta_{\rm KM}$ if we take $\delta V_{\rm CKM}$ into account).

With the presence of new physics, the B_s–$\overline{B}_s$ oscillation could be affected. Both the modulus and the phase of the oscillation amplitude would deviate from the Standard Model predictions. The values of ρ and η extracted from $\Delta m_{B^0}/\Delta m_{B_s}$ and $\Gamma_{b\to u+W}$ would be different from the CKM parameters $\rho_{\rm CKM}$ and $\rho_{\rm CKM}$.

The phase the B_s–$\overline{B}_s$ oscillation amplitude can be measured by the CP asymmetry in B_s and $\overline{B}_s \to J/\psi\phi$ decays. This measurement could still be compatible with the Standard Model prediction, if the contribution of new physics to the oscillation phase is small. It has to be noted that $J/\psi\phi$ can have CP $= +1$ and CP $= -1$ depending on the relative angular momentum between J/ψ and ϕ and their fractions must be determined experimentally in order to determine the phase of B_s–$\overline{B}_s$ oscillation amplitude from the measured CP asymmetry.

If CP violation in B_s and $\overline{B}_s$ decaying into $D_s^+ K^-$ and $D_s^- K^+$ are measured, the four time-dependent decay rates provide $\gamma_{\rm KM}$ in the Standard Model. This result remains unchanged if the contribution of new physics to the oscillation phase is small. However, $\gamma_{\rm KM}$ is different from $\tilde{\gamma}$ determined from $\tilde{\rho}$ and $\tilde{\eta}$ *i.e.* a clear discrepancy from the Standard Model prediction.

In summary, measurements beyond the CP asymmetry in B^0 and $\overline{B}^0 \to J/\psi K_S$ decays are needed in order to reveal new physics.

Due to the large contribution from the penguin diagrams in the decay amplitude, the CP asymmetry in B^0 and $\overline{B}^0 \to \pi^+\pi^-$ decays is no longer considered to be ideal to determine $\beta + \gamma$ even within the framework of the Standard Model. Such hadronic effects can be eliminated by measuring CP violation in B^0 and $\overline{B}^0 \to \rho\pi$ decays. However, the method still assumes that the $\pi\pi$ pairs always behave like ρ. New physics could affect significantly the $b \to d$ penguin diagrams. This complicates analysis of CP violation measurements in B^0 and $\overline{B}^0 \to \rho\pi$ decays.

It must be noted that additional measurements from the kaon system such as $K^\pm \to \pi^\pm \nu\overline{\nu}$ and $K_L \to \pi^0 \nu\overline{\nu}$ decays can provide independent information on ρ and η.

3. Experimental considerations

As shown in the previous section, many of the interesting decay modes are with pure hadronic final states. Therefore, the trigger system must be sensitive not only to the final states including leptons but also to the pure hadronic final states.

For precision measurements, background in the reconstructed final states must be reduced as much as possible. For some decay modes such as $B^0 \to \pi^+\pi^-$, other two-body decay modes of B mesons like $B^0 \to K^+\pi^-$ are the serious background. They can be reduced only by identifying particles.

The oscillation frequency of B_s–$\overline{B}_s$ is expected to be very high. Furthermore, CP violation is measured from the amplitude of the oscillation. In order to measure CP asymmetries with small uncertainty, a very good decay time resolution is required.

It is very likely that the CP asymmetry in B^0 and $\overline{B}^0 \to J/\psi K_S$ will be measured by the existing experiments at both e^+e^- B factories and hadron machines. However, they cannot measure well all the other decay modes described in the previous section. Expected CP violation effects in B^0 and $\overline{B}^0$ decaying into $D^{*+}n\pi$ and $D^{*-}n\pi$ are very small, requiring higher statistics than the existing machines can deliver. The B_s meson physics at e^+e^- factories is limited since this requires a special run at $\Upsilon(5S)$ and only with limited decay time resolution. D0 and CDF at the Tevatron collider do not have sufficient particle identification capabilities.

The cross section of the $b\bar{b}$ quark pairs at the LHC energy is estimated to be $\sim 500\ \mu$b; far larger than at any existing machines. The fraction of events with b quarks, $\sigma_{b\bar{b}}/\sigma_{\rm inelastic}$, is about 5×10^{-3} which is similar to the fraction of charm events in the present fixed-target charm experiments. Thus, LHC appears to be a very promising place to perform high precision CP violation measurements in B-meson decays. B_s, $\overline{B}_s$, $B_c^{\pm}$ and b-baryons are also abundantly produced, in addition to $B^{\pm}$, B^0 and $\overline{B}^0$.

The LHCb detector is designed to fulfil all the detector requirements listed above so that the potential of the LHC can be fully exploited.

4. LHCb spectrometer

Figure 2 illustrates the LHCb spectrometer [7]. It resembles a typical fixed target spectrometer, consists of a vertex detector at the intersection point (placed in "Roman pots"), a tracking system, RICH counters with aerogel and gas radiators, a large-gap dipole magnet, a calorimeter system, and a muon system.

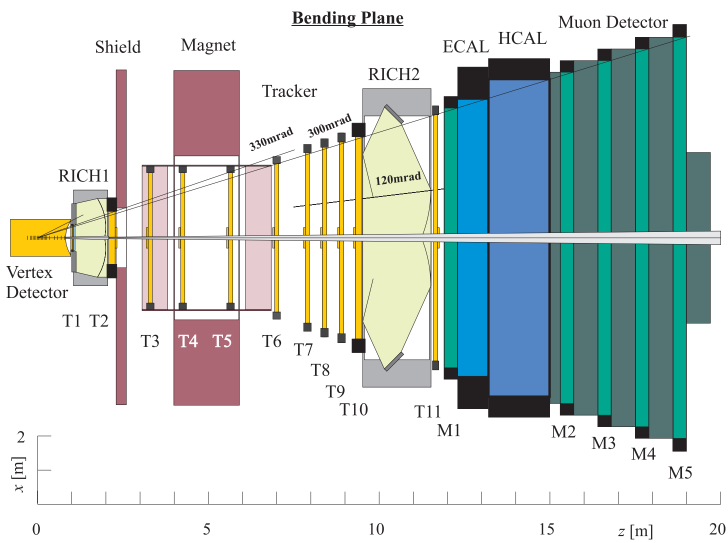

Fig. 2. The LHCb spectrometer

The choice of the detector geometry is based on the fact that both the b- and $\bar{b}$-hadrons are predominantly produced in the same forward cone at high energies. This feature is essential for the flavour tag. Figure 3 shows the polar angles of the b- and $\bar{b}$-hadrons obtained by the PYTHIA simulation programme. The polar angle is defined with respect to the beam axis in the pp center-of-mass system.

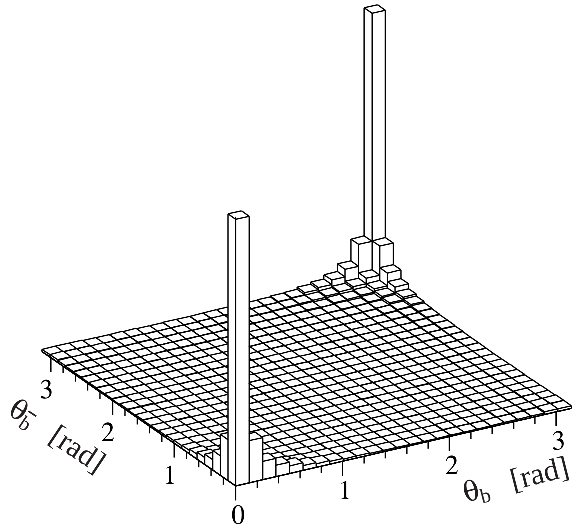

Fig. 3. Polar angles of the b- and $\overline{b}$-hadrons obtained by the PYTHIA simulation programme.

IP-8, the experimental area currently occupied by the DELPHI experiment, will be used for the LHCb experiment. At IP-8, the pp collision point will be displaced by ~ 11 m so that large detector components such as the magnet, calorimeters and muon system can be placed in the already existing hall. Therefore, no extra excavation is required.

4.1. Beam pipe

A 1.8 m long section of the beam pipe around the interaction point has a large diameter of approximately 120 cm. This accommodates the vertex detector system with its retraction mechanics, and has a thin forward window over the full detector acceptance. This part is followed by two conical sections; the first 1.5 m long with 25 mrad opening angle, and the second 16 m long with 10 mrad opening angle.

4.2. Magnet

The spectrometer dipole magnet is placed right after RICH-1. A superconducting magnet is chosen to obtain a high field integral of 4 Tm with a short length. The polarity of the field can be changed to reduce systematic errors in the CP-violation measurements that could result from a left-right asymmetry of the detector. An iron shield upstream of the magnet reduces the stray field in the vicinity of the vertex detector and of RICH-1.

4.3. Vertex detector

A total of 19 layers of silicon microstrip detectors are placed perpendicular to the beam, of which 17 layers are used as a vertex detector system. The remaining two layers are dedicated for detecting bunch crossings with more than one pp interactions as a part of the Level-0 trigger (pile-up veto counter). Each layer of the vertex detector system consists of two planes with r and ϕ strips respectively. The r-strips provide azimuthal and the ϕ-strips radial coordinates. Pile-up veto counters consist of ϕ-strip planes only. These strip configurations are chosen to make an efficient trigger algorithm. The closest distance between the active silicon area and the beam is 1 cm. The silicon detectors are placed in Roman pots with 100 mm thick aluminium windows, which act as a shield against RF pickup of the circulating beams. In order to avoid collapse of the windows, a secondary vacuum is maintained inside the Roman pots. During the injection and acceleration, the Roman pot system will be moved away from the beam to avoid interference with the machine operation and accidental irradiation of the detectors.

4.4. Tracking system

Because of the high particle density close to the beam pipe, the LHCb tracking detector is split into inner and outer systems. The inner tracking chambers have dimensions of 60×40 cm^2. Drift chambers based on Straw technology are considered as baseline for the outer tracking detector. For the inner tracking system where high granularity is required, Micro Cathode Strip Chambers (MCSC's) with Gaseous Electron Multipliers (GEM's) are taken as the base-line technology.

4.5. RICH detectors

The RICH system of the LHCb detector consists of two detectors with three different radiators in order to cover the required momentum range, 1–150 GeV/c. The first detector uses aerogel and C_4F_{10} gas as radiators. The second detector, used for high momentum particles, is placed after the magnet and uses CF_4 as the radiator. The Cherenkov light is detected with planes of Hybrid Photon Detectors (HPD's) placed outside the spectrometer acceptance.

4.6. Calorimeter system

The calorimeter system consists of a preshower detector followed by electromagnetic and hadronic calorimeters. It also serves as the initial part of the muon filter system. The cells of the Preshower detector are made up from

14 mm thick lead plates followed by square scintillators, 10 mm thick. Transverse dimensions match the segmentation of the electromagnetic calorimeter. For the electromagnetic part, a Shashlik calorimeter is used since a rather modest energy resolution is required. The hadron calorimeter is based on a scintillating tile design similar to that used in the ATLAS experiment. The required energy resolution is less severe than for ATLAS. The inner acceptance of the calorimeter system starts at 32 mrad from the beam in the bending plane of the spectrometer dipole, and 27 mrad in the non-bending plane.

4.7. Muon system

The technology considered for the muon stations are Multigap Resistive Plate Chambers (MRPC's) for most of the coverage and Cathode Pad Chambers (CPC's) for regions where the expected rate exceeds 5 kHz/cm^2. The readout pad structure is optimized for the trigger purpose.

4.8. Trigger

The LHCb trigger is based on four decision levels. Due to the large mass and the transverse momentum spectrum of the B-meson, its decay products have on average higher p_{T} than particles produced in most of the inelastic pp interactions (minimum-bias events). Decay products of the B meson originate from vertices that are displaced from the primary interaction point by several millimetres. The early levels of the LHCb trigger exploit those two characteristics. Level-0 decision is based on high-p_{T} hadrons or electrons found in the calorimeter system or muons found in the muon system. It provides a modest reduction of minimum-bias events by a factor of ~ 10. At Level-1, data from the vertex detector are used to select events with multiple vertices. Level-1 provides a reduction factor of ~ 25 for minimum-bias events. After a positive decision of the Level-1 trigger, data are read out to an event buffer. Hereafter, all the detector information is in principle available for the trigger decision. At Level-2, a further enhancement of events with b-hadrons is achieved by combining different detector components; for example by refining the reconstruction of the b-hadron decay vertices using momenta measured in the tracking system and information from the vertex detector. At Level-3, the trigger decision is made by reconstructing the full event. Due to the large b-hadron production rate, not all the events with b-hadrons can be recorded. Therefore, the b-hadron final states are reconstructed to select only the decay modes of interest.

5. Important characteristics of the LHCb detector

The benefit of having particle identification and good invariant mass resolution can be best demonstrated by reconstructing $B_s \to D_s^+ K^-$ decays. The worst background to this decay mode comes from $B_s \to D_s^+ \pi^-$ decays which are used to study B_s–$\overline{B}_s$ oscillations. Compared to this decay mode, the branching fraction of $B_s \to D_s^+ K^-$ is suppressed by a factor of $1/\lambda^2 \approx 20$. Only the invariant mass resolution and particle identification will help to reduce this background. It should be noted that momenta of K^- and π^- from these decay modes are large since they are two-body decays.

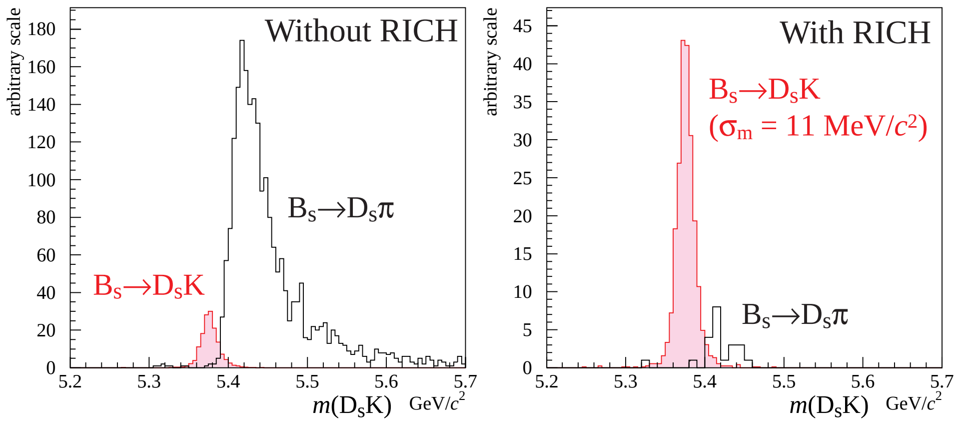

Fig. 4. The LHCb simulation results for the reconstructed invariant mass distributions for $D_s^+ K^-$ combinations without and with particle identification using RICH.

Figure 4 shows the reconstructed invariant mass distributions expected with the LHCb detector for $D_s^+ K^-$ combinations without and with particle identification using RICH. With the combination of the good mass resolution ($\sigma = 11$ MeV/c^2) and RICH particle identification, the background from $B_s \to D_s^+ \pi^-$ decays can be completely removed in the reconstructed $D_s^+ K^-$ sample. It should be noted that no CP violation effect is expected in the background decay mode. The decay time resolution is found to be 43 fs.

The LHCb trigger system is designed to cope with the rather small $\sigma_{b\bar{b}}/\sigma_{\text{inelastic}}$ of $\sim 5 \times 10^{-3}$ at the LHC energies, still maintaining a high efficiency for events with b hadrons. The strategy is to spread the suppression factors evenly and not to rely on a particular trigger selection, in particular at early levels where available information from the detector is limited, reflecting in the modest suppression factors of 10 and 25 for the ordinary pp interaction events by the Level-0 and Level-1, respectively. Simulation results of the trigger performance can be relied upon for such a modest suppression. By not heavily relaying on a particular selection criterion, the trigger system is flexible and can be readjusted to the yet unknown running conditions of the experiment.

With the particle identification capability, an effective flavour tag can be obtained using the charged kaons from the b hadron decays. No lepton is required in the analysis for flavour tagging. Therefore, the Level-0 hadron high p_{T} trigger increases significantly the statistics of the sample with pure hadronic B decay final states compared with the lepton high p_{T} trigger alone. Table I summarises the Level-0 trigger efficiencies for various decay modes. Efficiencies are calculated for those events where the initial flavour is identified and the final state is fully reconstructed with all the cuts applied to remove background. While $J/\psi K_S$ final states are mainly triggered by the muon and electron high-p_{T} triggers, the hadron high-p_{T} trigger is essential for the hadronic final states.

TABLE I

Level-0 trigger efficiencies for reconstructed and flavour tagged final states

Decay Mode	Level-0 high-p_{T} muon	Level-0 high-p_{T} electron	Level-0 high-p_{T} hadron	Level-0 all combined
$B^0 \to J/\psi(e^+e^-)K_S$	0.17	0.63	0.17	0.72
$B^0 \to J/\psi(\mu^+\mu^-)K_S$	0.87	0.06	0.16	0.88
$B_s \to D_s^+K^-$	0.15	0.09	0.45	0.54
$B^0 \to \pi^+\pi^-$	0.14	0.08	0.70	0.76

The table also indicates that the Level-0 trigger efficiencies are very high for those events useful in the analysis. As a result, the LHCb experiment will run with a luminosity of 2×10^{32} cm^{-2}s^{-1} and still collect 2.4 k reconstructed and initial flavour tagged B_s and $\overline{B}_s$ decays into $D_s^+K^-$ and $D_s^-K^+$. This luminosity is far below the design luminosity of 10^{34} cm^{-2}s^{-1} and should be reached from the beginning of the LHC operation. At this luminosity, the bunch interactions are dominated by events with only one pp collision. The running luminosity will be locally tuned at the LHCb intersection such that the experiment can run with this optimal luminosity while the other LHC experiments run at the design luminosity. It must be noted that running at lower luminosities has an additional benefit that the radiation damage of the detector is reduced.

6. Summary

Precision studies of CP violation could reveal physics beyond the Standard Model. The B-meson systems are particularly suited for such studies since theoretical uncertainties in the Standard Model predictions can be well understood in some decay modes. Hadronic effects are either not present or can be measured experimentally.

$B^0 \to J/\psi K_S$ is a such decay mode. However, this decay mode alone is not sufficient to test whether new physics is present in addition to the Standard Model. By measuring other decay modes such as $B^0 \to D^{*+} n\pi$ and $B_s \to D_s^+ K^-$, the experiment would become sensitive to new physics.

With the current generation of experiments, precise CP violation measurements in those decay modes cannot be done due to either lack of statistics or limitations of the detectors. LHC will give a sufficient number of B mesons. In addition, the LHCb detector will be required in order to fully exploit the large number of B mesons from the beginning of the LHC operation. This is due to the efficient and flexible trigger, particle identification capability and very good mass and decay time resolutions.

The author thanks to the organizers of this meeting for their hospitality. R. Forty is acknowledged for his careful reading of this manuscript.

REFERENCES

[1] A.D. Sakharov, *JETP Lett.* **6**, 21 (1967).
[2] See for example M.B. Gavela *et al.*, *Mod. Phys. Lett.* **9A**, 795 (1994).
[3] N. Cabibbo, *Phys. Rev. Lett.* **10**, 531 (1963); M. Kobayasi, K. Maskawa, *Prog. Theor. Phys.* **49**, 652 (1973).
[4] L. Wolfenstein, *Phys. Rev. Lett.* **51**, 1945 (1983).
[5] C. Caso *et al.*, (Particle Data Group), *Euro. Phys. J.* **C3**, 1 (1998).
[6] Nice overview on CP violation in B-meson decays can be found in *The BaBar Physics Book*, eds P.F. Harrison and H.R. Quinn, SLAC-R-504, 1998.
[7] S. Amato *et al.*, LHCb Technical Proposal, CERN/LHCC 98-4, 1998.